ATP induced photoreceptor death in a feline model of retinal degeneration

Felix P. Aplin[1,2,3], Chi D. Luu[1], Kirstan A. Vessey[2], Robyn H. Guymer[1], Robert K. Shepherd[3,4], Erica L. Fletcher[2]

[1]Centre for Eye Research Australia, The University of Melbourne, Royal Victorian Eye & Ear Hospital, East Melbourne, Victoria 3002, Australia; [2]Department of Anatomy and Neuroscience, The University of Melbourne, Melbourne, Victoria 3010, Australia; [3]The Bionics Institute, East Melbourne, Victoria 3002, Australia; [4]Medical Bionics Department, The University of Melbourne, Melbourne, Victoria 3010

Running title: A feline model of retinal degeneration

Word count:

Abstract: 223 Text: 5145 Number of pages: 23 Number of figures: 9

Author for correspondence:
A/Prof Erica Fletcher
Department of Anatomy and Neuroscience
University of Melbourne
Victoria, 3010
Australia
Telephone number: +61 –3 83443218
Fax number: +61 –3 93475219
E-mail address: elf@unimelb.edu.au

Grant support: This work was supported by the Australian Research Council (ARC) through its Special Research Initiative (SRI) in Bionic Vision Science and Technology grant to Bionic Vision Australia (BVA) and by the NHMRC project grant (APP1021042; APP1061419) to ELF by Retina Australia. CERA receives Operational Infrastructure Support from the Victorian Government and is supported by NHMRC Centre for Clinical Research Excellence Award 529923.

Abstract

Purpose: To develop and characterize a feline model of retinal degeneration induced by intravitreal injection of adenosine tri-phosphate (ATP).

Methods: 19 normally sighted adult cats received 100 µL intravitreal injections of ATP with a final concentration of 11 mM, 22 mM or 55 mM at the retina. Four animals were sacrificed 30 hours after injection and retinal sections examined for apoptosis using a TUNEL cell death assay. In remaining animals, structural and functional changes were characterized over a 3 month period using a combination of electroretinography (ERG) and optical coherence tomography (OCT).

Results: Using a TUNEL cell death assay, we detected widespread photoreceptor death 30 hours after injection with 55 mM intravitreal ATP. All concentrations of ATP caused loss of retinal function and gross changes in retinal structure within 2 weeks of injection. Intravitreal injection of ATP lead to a rapid loss of rod photoreceptor function and a gradual loss of cone photoreceptor function within 3 months. Outer nuclear layer thickness was globally reduced by 3 months, with the inner nuclear layer including the retinal nerve fiber layer remaining intact. Structural abnormalities were observed including focal retinal detachment with evidence of both intravitreal and intraretinal inflammation in some eyes.

Conclusions: Development of an ATP-induced feline model of retinal degeneration provides a rapid and effective large-eyed animal model for research into vision restoration.

Key words: Retinitis pigmentosa, animal model, feline, photoreceptor, retinal degeneration

Introduction:

Photoreceptor death accounts for more than 50% of cases of blindness, contributing to the disease progression of inherited retinal degenerations such as Retinitis pigmentosa (RP)[1] and Age Related Macular Degeneration. Although the underlying cause(s) of photoreceptor death varies in these conditions, they are characterised by progressive loss of photoreceptors with functional and structural changes occurring at later stages in the inner retina[2-6]. Over recent years there have been significant advances in the development of visual restorative therapies including photoreceptor transplantation, gene therapy, optogenetic approaches and electronic implantable devices[7-10]. Animal models are an essential part of this research as they allow for proof of principle and the testing of safety and efficacy for new technologies, such as visual prostheses[11, 12].

Development of restorative strategies benefit from the use of animal models that mimic the anatomical size and structure of a human eye[11]. Many such animal species develop inherited retinal degenerations including Abyssinian cats[13, 14], Briard dogs[15, 16], and Irish setters[17]. In addition, transgenic pigs and rabbits have been developed[18-20]. Studies using these animals are limited by availability, high cost and often slow rate of photoreceptor loss. Pharmacological methods of retinal degeneration such as sodium iodate[21], N-methyl-N-nitrosourea[22] (MNU) and adenosine tri-phosphate[23, 24] (ATP) may provide an alternative approach as they tend to have a faster time-course and are cheaper than comparable transgenic models. To this end we decided to pursue the development of an ATP-induced model of photoreceptor degeneration in cat via intraocular injection as this would

allow us to selectively reduce vision in one eye of the animal without any systemic side effects.

ATP is ubiquitous within the body and acts as an intracellular energy transport molecule. In the central and peripheral nervous system extracellular ATP also acts as a neurotransmitter[25]. ATP activates two classes of purinergic receptors known as the P2X (ligand-gated cationic channel) and P2Y (G protein-coupled receptors) receptor types. Very large concentrations of extracellular ATP can lead to cell death within central nervous system neurons via the action of the purinergic receptor $P2X_7$[26, 27]. Whilst the exact mechanism of cell death is still not completely understood, it is possible that chronic activation of the $P2X_7$ receptor causes a rapid influx of calcium ions into the cell, triggering apoptosis[23, 26, 28]. $P2X_7$ receptors are present both pre and post-synaptically in both the inner and outer plexiform layers of the retina[29, 30], and the addition of high doses of extracellular ATP beyond physiological limits leads to photoreceptor death[23, 24] Other retinal neurons appear to be resistant to ATP-induced cell death except at very high concentrations, possibly due to a neuroprotective effect from the adenosine receptor A3[31-33].

Although the time course and characteristics of ATP induced degeneration have been well described in rats[23, 24], it has never been tested in other animal models. To this end the aim of this study was to characterise the effects of intravitreal injection of ATP in a feline model over a three month period. We chose a feline model because the eye is of similar size to humans[34], the retina and visual cortex are well described and are they are the most commonly used large-eyed animal model in visual prosthesis research[11].

Materials and methods:

Anaesthesia and Intraocular injection of ATP in cat:

Normally sighted adult laboratory cats (n = 19) were utilized in this study. Treatment of animals complied with the Association for Research in Vision and Ophthalmology Statement for Use of Animals in Ophthalmic and Vision Research, and the National Health and Medical Research Council's ''Australian Code of Practice for the Care and Use of Animals for Scientific Purposes'' (2013) and the ''Prevention of Cruelty to Animals Act'' (1986; and amendments). All studies were approved by the Royal Victorian Eye and Ear Hospital Animal Ethics Committee (RVEEH AEC; #10/200AB, #12/256AB).

Intravitreal injection of ATP was performed under anaesthesia using a combination of ketamine (20mg/kg, Ilium Ketamil, Troy Laboratories, NSW, Australia) and xylazine (2mg/kg, Ilium Xylazil-20, Troy Laboratories, NSW, Australia) injected subcutaneously. In order to maintain normal intraocular pressure, an anterior chamber paracentesis was performed using a 30G needle and approximately 50µL of aqueous humour tapped from the anterior chamber. A solution containing 100 µL of either 0.2M, 0.4M or 1M adenosine tri-phosphate hydrate (Sigma Pharmaceuticals, VIC, Australia) and 0.2 mg dexamethasone to control intravitreal inflammation (4mg/ml, Dexamethasone, Aspen Australia, NSW, Australia) in sterile phosphate buffered saline (PBS, 0.9%) was injected with a 30G needle into the vitreous of one eye. The other eye received either a sham injection of 0.2mg dexamethasone in 0.9% PBS (n=9) or no injection (n=8). A peri bulbar injection of 50 µL methylprednisolone acetate (40mg/mL, Depomedrol, Pfizer Australia, NSW,

Australia) was given following the intravitreal injection of ATP or saline to relieve extra-ocular inflammation at the injection site. At the completion of the injection procedure, cats were rehydrated with Hartmann's solution (2.5 ml/kg/h; subcutaneous) and allowed to recover. Analgesic (buprenorphine 0.01 mg/kg; subcutaneous; Temgesic; Reckitt Benckiser, Sydney, Australia) was administered post operatively. For one week following surgery, topical antibiotics (Chlorsig; Sigma Pharmaceuticals, VIC, Australia) and corticosteroids (Predneferin Forte; Sigma Pharmaceuticals, VIC, Australia) were administered twice daily. Animals were monitored by research and animal care staff daily, and received weekly visits from a veterinarian. Based on an estimated 2.7 mL vitreal volume in the cat[34], concentrations of 0.2M, 0.4M and 1M ATP corresponded to 11mM, 22mM and 55mM ATP at the retina after diffusion through the vitreous.

Clinical assessments

Retinal function and structure in 15 of the ATP injected animals was assessed 2, 6 and 12 weeks post ATP injection. Animals were anaesthetised with a subcutaneous dose of ketamine (20mg/kg) and xylazine (2mg/kg). Depth of anaesthesia was monitored via corneal reflex and respiratory rate; if the anaesthesia became too light during assessment, animals were injected with a further one-third standard dose of ketamine and xylazine. During assessment the cornea was kept hydrated using topical application of a sterile saline solution (0.9%). Pupils were dilated with 1% tropicamide (Chauvin Pharmaceuticals, Surrey, England) and 2.5% phenylephrine hydrochloride (Chauvin Pharmaceuticals, Surrey, England). With the exception of the terminal time point, subjects were rehydrated with Hartmann's solution (2.5 ml/kg/h;

subcutaneous) at the end of the assessment and allowed to recover. All assessment methodologies performed on these animals have been previously described in normally sighted cats and other animal models of photoreceptor degeneration[12, 35-38].

Electroretinogram:

Retinal function was assessed using a full-field flash ERG (Espion, Diagnosys LLC, Lowell, MA, USA) after 30 minutes of dark adaptation. Both the ATP injected and the fellow control eyes were recorded simultaneously using corneal Jet electrodes. In each animal the retinal response to stimulus intensities from 0.001 to 10 cd.s/m^2 were recorded. However, only the combined rod-cone maximal ERG response (10 cd.s/m^2) is reported here. In 11mM injected animals, a twin flash paradigm consisting of two consecutive flashes (10 cd.s/m^2, 500ms inter stimulus interval) was used to assess rod and cone responses independently. The first flash elicited a mixed response from both rod and cone photoreceptors, whilst the second flash elicited responses only from cones[39, 40]. Rod responses were isolated digitally via subtraction of the cone response from the mixed response. Rod and cone pathway a-wave amplitudes corresponding to the photoreceptoral response[41, 42] were measured from the pre-stimulus baseline to the a-wave trough. The b-wave amplitudes corresponding to the post-receptoral response[41, 42] were measured from the a-wave trough to the b-wave peak. Implicit times were measured from the time of the flash presentation to the maximal amplitude of a-wave and b-wave responses. Oscillatory potentials (OPs), corresponding to several distinct post-receptoral responses including amacrine cell output[43], were also recorded using a band-pass filter between 100-300Hz and analysed separately. OP amplitude and implicit time was

177 determined by measuring the amplitude of each individual OP from baseline. Only
178 OPs1-4 could be reliably measured from our data due to the low amplitude of OP5 in
179 normally sighted animals.

180

181 ***Ocular Coherence tomography acquisition and analysis:***

182 Retinal structure was analysed in ATP injected and fellow control eyes using a
183 Fourier domain Ocular Coherence tomography (OCT) (Spectralis, Heidelberg
184 Engineering GmbH, Heidelberg, Germany). In order to assess retinal structures, high
185 resolution line scans were taken at each time point across the temporal retina, area
186 centralis and nasal retina. In order to assess thickness of the retinal nerve fibre layer,
187 a high resolution circular scan was taken around the optic nerve. Each scan was a
188 composite image average from 100 frames. Figure 1a and 1b show representative
189 infrared reflectance images of the fundus displaying length and location of scans
190 performed in each eye. Figure 1c and 1d show representative OCT b-scan images
191 taken from a temporal (Fig. 1c) and circular (Fig. 1d) scan. Images were exported as
192 tagged image files (.TIF) and retinal thicknesses were measured using custom
193 software in ImageJ (version 1.48; National Institutes of Health, Bethesda, MD). Line
194 scan images were separated into three distinct thickness measurements as shown in
195 Figure 1c, defined as total retina (inner limiting membrane to border of retinal
196 pigment epithelium (RPE) and tapetum lucidum), inner retina (inner limiting
197 membrane to outer plexiform layer) and outer retina (outer plexiform layer to border
198 of RPE and tapetum). Circular scan thicknesses were separated as shown in Figure
199 1d into total retina, retinal nerve fibre layer (RNFL, inner limiting membrane to

ganglion cell layer) and ganglion cell layer plus all subsequent retinal layers (GCL+, ganglion cell layer to Bruch's membrane).

Tissue collection and fixation:

At 30 hours after intravitreal injection with ATP, animals (n=4) were deeply anaesthetized using ketamine (20mg/kg) and xylazine (2mg/kg) and then euthanized with an overdose of sodium pentobarbitone (150mg/kg, intra-cardiac). The eyes were enucleated and tissue anterior to the ciliary body dissected away. The remaining tissue was fixed in 4% paraformaldehyde for 30 minutes. After this period, the tissue was washed in phosphate buffered solution (PB), dissected and then equilibrated in graded solutions of sucrose (10%, 20% w/v in PB) for at least 30 minutes each and finally placed in 30% sucrose overnight. Control and ATP-treated tissue were embedded in optimal cutting temperature compound (Tissue-Tek, Sakura, Torrance, CA), frozen and cut at 12 μM on a cryostat (Microm, Walldorf, Germany). Sections were collected on Poly-L-lysine coated slides (Menzel-Glaser, Braunschweig, Germany) and stored at -20˚C until use.

Cell death assay:

Cell death was measured using a commercially available fluorometric terminal dUTP nick-end labelling (TUNEL) kit (DeadEnd Fluoro metric TUNEL system, TB235; Promega, Madison, WI) in a method identical to a previous study of ATP induced degeneration in rat[23]. Using a Cryostat, 12μM sections of retina were taken both near the area centralis (~3 optic disk diameters temporal to the optic nerve) and in

the peripheral temporal retina. Sections were washed twice for 5 minutes in 0.9% PBS before being digested with 0.5% Triton-X in PBS for 5 minutes. Sections were then washed in PBS three more times for 5 minutes and equilibrated using equilibration buffer (200 mM potassium cacodylate, pH 6.6; 25 mM Tris-HCl, 0.2 mM DTT, 0.35 mg/ml bovine serum albumin [BSA], 2.5 mM cobalt chloride) for 10 minutes. A reaction mix (equilibration buffer, 50 µM fluorescence-12-dUTP, 100 µM dATP, 10 mM Tris-HCl, 1mM EDTA, rTdT enzyme) was applied to the sections for one hour at 37˚ C in darkness. This reaction was stopped using an SSC buffer (0.3 M sodium chloride, 0.15M sodium citrate, pH 7.2) and the sections rinsed with PBS an additional three times for 5 minutes. Sections were coverslipped with a Mowiol based anti-fade mounting medium and photomicrographs taken on a laser scanning confocal microscope (Carl Zeiss, Göttingen, Germany) with air objectives at 20x and 10x magnification. Apoptotic cells were quantified manually using a cell counter application (ImageJ, version 1.48; National Institutes of Health, Bethesda, MD) with 5 regions per section at 1 mm length each.

Statistical analysis:

Analyses were performed on TUNEL cell counts, ERG and OCT thickness data in eyes injected with ATP compared to control and PBS sham injected eyes (Graphpad Prism v.4, San Diego, CA, USA; SigmaPlot v12.5, Systat Software, San Jose, CA). Results are expressed as the mean ± standard error of the mean (SEM). All data was analysed via a Shapiro-Wilk test for normality. Changes in cell counts, ERG responses and OCT thickness with ATP concentration or time post-injection were analysed by one-way analysis of variance (1-way ANOVA) or Kruskal-Wallis one-

247 way analysis of variance by ranks (Kruskal-Wallis), dependent on normality. A Holm-
248 Sidak post-hoc test was used to determine significance for multiple pairwise
249 comparisons. The interaction between ERG oscillatory potential amplitudes, b-wave
250 and a-wave amplitudes were determined using a Deming regression. Details of
251 individual tests used are also provided in the results. In all figures, statistical
252 significance is expressed as * ($P < 0.05$).

253

Results:

Intravitreal injection of ATP causes photoreceptor degeneration in cat

The purpose of this study was to characterize the effect of intravitreal injection of ATP on the cat retina. It was first necessary to determine whether intravitreal injection of ATP led to acute and specific photoreceptor degeneration in cat as it does in the rat[23, 24]. We injected 55 mM ATP into the vitreous of 4 cat eyes and assessed the level of cell death 30 hours later using a TUNEL assay. Figure 2 shows vertical sections of retinae from PBS injected central retina (Fig. 2a) and ATP injected central (Fig. 2b) and peripheral (Fig. 2c) retina that were labelled for TUNEL. In order to determine whether the extent of cell death varied between ATP and PBS injected eyes TUNEL positive nuclei were quantified per mm of retinal section (Fig. 2d) and as a proportion of total ONL nuclei per mm^2 (Fig. 2e). There was a significant difference between saline (0.01 cells/mm, data not shown) and ATP injected eyes (1-way ANOVA; $P < 0.01$; $n = 4$). The total number of TUNEL positive nuclei in ATP injected eyes did not vary significantly with location (1-way ANOVA; $P > 0.05$; $n = 4$). A similar proportion of ONL nuclei were TUNEL labelled in both central and peripheral retina ($P > 0.05$). Very few TUNEL positive cells were present in other layers in ATP treated eyes (average 0.24 TUNEL positive cells per mm of retina, or less than 0.01% of inner retinal cells) and none in PBS injected eyes. These data confirm that high concentrations of intravitreal ATP leads to widespread photoreceptor specific cell death within 30 hours of injection in cat.

To investigate the optimal concentration of ATP that induced photoreceptor degeneration reliably in the cat we injected a total of 15 animals with intravitreal ATP

at concentrations of 11, 22 or 55 mM at the retina and PBS sham injection in the contralateral eye. Retinal structure and function was assessed using temporal OCT scans and dark adapted ERG two weeks following injection. Figure 3a shows representative ERG response waveforms two weeks after injection with ATP or in control eyes. Representative waveforms are not shown for the PBS condition as they were identical to the control waveforms. As shown in Figure 3b, ATP caused a significant loss of photoreceptor function irrespective of the concentration injected (Kruskal-Wallis; $P < 0.05$; n = 3 for 22mM injected eyes; 4 for 11mM, 55mM and sham injected eyes; 8 for control eyes). The amplitudes of the b-wave were similarly affected (Fig. 3c; Kruskal-Wallis; $P < 0.05$; n = 3-8). Representative extracted OP waveforms are shown in Figure 3d. Summed OP amplitudes did not differ between control and PBS sham conditions ($P > 0.05$) but were significantly reduced at all ATP dosages compared to the control (Fig. 3e; $P< 0.05$).

Figure 4 shows representative OCT images and a quantification of total retinal thickness across the temporal retina following injection with either ATP or PBS. Injection of 55 mM ATP induced significant reduction of total retinal thickness compared to controls and 11 mM ATP injected eyes (Fig. 4e; Kruskal-Wallis; $P < 0.05$; n = 3 for 22mM injected eyes; 4 for 55mM injected eyes; 8 for control, sham and 11mM injected eyes). All other concentrations were not significantly different from controls ($P > 0.05$). We evaluated retinal integrity in all animals, and observed a number of retinal detachments (white arrows in Figure 4). Detachments resolved in cats injected with 11mM ATP but worsened over time in cats injected with 22mM and 55mM ATP. Therefore, the 11mM ATP concentration was selected as the ideal dose for subsequent chronic experiments. As no differences in function or structure were

observed between control and PBS eyes, the two groups are combined in all subsequent experiments.

ATP induces rapid loss of rod and progressive loss of cone function.

The time course of rod and cones degeneration in cats injected with 11mM ATP was examined using a twin flash ERG at baseline, and following 2, 6 and 12 weeks after injection. Representative waveforms of rod isolated responses at various time points post ATP injection are shown in Figure 5a. Rod a-wave amplitude (Fig. 5b) was significantly reduced by 2 weeks post injection (1-way ANOVA; $P < 0.05$; $n = 8$ for 11mM injected eyes; 13 for control eyes). Although there was a trend of continued rod a-wave loss towards 12 weeks, the difference between ATP injected time points was not statistically significant. Rod b-wave amplitudes (Fig. 5c) were similarly reduced by 2 weeks following injection ($P < 0.05$). Representative waveforms of cone responses are shown in Figure 5d. Cone a-wave amplitude (Fig. 5e) showed a different rate of degeneration, with significant loss from baseline only occurring at the 12 week time point ($P < 0.05$). Cone b-wave amplitudes (Fig. 5f) were significantly reduced by 6 weeks ($P < 0.05$).

In the early stages of retinitis pigmentosa, oscillatory potential amplitudes appear to be reduced at a comparatively slower rate than a-wave amplitudes[44]. In order to explore this relationship in our model, oscillatory potentials were analysed separately (Fig. 6). Figure 6a shows representative OP response waveforms. Figure 6b shows summed OP amplitudes at each time point. OPs were significantly reduced from two

weeks post injection (1-way ANOVA; $P < 0.05$; n= 8-13). In order to evaluate whether ATP affected the OPs to a greater extent than the a-wave we correlated the amplitude of the mixed a-wave with the amplitudes of the summed OPs and mixed b-wave. As shown in Figure 6c, the amplitude of the a-wave correlates with the amplitude of the OPs in controls (Deming regression; $P <0.01$; n = 8-13). However, two weeks after ATP injection, the slope of the correlation is altered (Deming regression; $P <0.05$; n = 8-13), suggesting that the OP amplitudes had decreased by a greater margin than a-wave amplitudes. Specifically, oscillatory potentials were reduced even in animals where the a-wave remained relatively intact. Figure 6d shows the correlation between the mixed a-wave and b-wave amplitudes. Amplitudes were significantly correlated at baseline and 2 weeks following ATP injection (Deming regression; $P < 0.05$; n = 8-13), and the slopes of the curves were no different (Deming regression; $P > 0.05$; n = 8-13), suggesting that any loss of the b-wave amplitude can be explained by losses in the a-wave.

ATP induced degeneration reduces outer retinal thickness and leaves inner retina intact

In view of the loss of the a-wave following ATP injection, the extent and nature of structural changes within the retina following ATP injection were examined. Figure 7 shows representative OCT images from regions within the temporal retina (7a), area centralis (7b), nasal retina (7c) and optic nerve head (7d) that were imaged at different times following injection. A thinned and inconsistent outer nuclear layer was clearly visible 12 weeks after injection in all retinal areas. The retina was also visibly thicker at 2 weeks when compared to the control. OCT images revealed multiple

localised retinal detachments at all time points (white arrows), many of which settled over the course of the 12 weeks. Hyper-reflective vitreous opacities (white asterisks), presumably corresponding to inflammatory cells in the vitreous, were occasionally seen at early time points but were not visible at 12 weeks.

In order to assess changes in retinal thickness following ATP injection, we analysed the thickness of total, inner and outer retinal components separately. Figure 8 shows thickness of the retina at different retinal eccentricities at each time point in temporal and optic nerve scans. The area centralis and nasal scan both showed similar thickness variation to the temporal scan. The temporal retina showed a reduction in total retinal thickness at 12 weeks after injection with ATP (Fig. 8a). Figure 8b and c show the inner (Fig 8b) and outer (Fig 8c) retinal thickness by eccentricity. The inner retina appeared to be thicker two and six weeks after ATP injection. In contrast, the outer retina is progressively thinner with increasing time after injection. There were no major variations in thickness across eccentricity. Using a circular scan to analyse the retina close to the optic nerve (Fig. 8d) revealed a pattern in thickness similar to other retinal areas, with a reduction at 12 weeks post injection). Analysis of the retinal nerve fibre layer (Fig. 8e) showed an altered profile in ATP-injected animals, but the conservation of average retinal thickness across the scan. Analysis of the neural retina (total area distal to the retinal nerve fibre layer, Fig 8f) showed that losses in total retinal thickness were primarily due to a thinning of the neural retina rather than loss within the RNFL, with no significant regional variation.

373 Having established no extreme variations in OCT thickness by eccentricity, we
374 quantified the mean thickness of the various regions of the retina from OCT images
375 (Fig. 9). Figure 9 shows the total (Fig. 9a), inner (Fig. 9b) and outer (Fig. 9c) retinal
376 thickness from the temporal, nasal and area centralis scans, averaged across the
377 retina and compared between time points. Total and outer retinal thickness were
378 significantly reduced at all locations by 12 weeks (Kruskal-Wallis; $P < 0.05$; $n = 8$).
379 The Inner retina had significantly increased in thickness at 6 weeks in the temporal
380 and nasal retina, but was reduced to baseline by 12 weeks (Kruskal-Wallis; $P < 0.05$;
381 $n = 8$). Across the area centralis, the inner retina thickened significantly from 2 weeks
382 (Kruskal-Wallis; $P < 0.05$; $n = 8$). Figure 9d shows circular scan thickness separated
383 into total retina, retinal nerve fibre layer (RNFL) and all other retinal layers (GCL+).
384 Total retinal and GCL+ thickness were significantly reduced by 12 weeks (Kruskal-
385 Wallis; $P > 0.05$; $n = 8$), but RNFL thickness remained unchanged (Kruskal-Wallis; P
386 < 0.05; $n = 8$). These results suggest that the majority of ganglion cells remain intact
387 at all stages following injection.

388

389

Discussion:

The major findings of this study were that intravitreal injection of ATP in a feline model leads to rapid photoreceptor death, similar to the effects described previously in the rat[23, 24]. In particular, our results show that ATP induces rapid loss of rods prior to cones, and that neurons of the inner retina remain relatively intact. These results suggest that ATP injection may be useful in creating a feline model of retinal degeneration.

ATP kills photoreceptors in cat:

Although ATP has been shown to kill photoreceptors in rat[23, 24], there have previously been no studies to determine the viability of this model in an animal model with an eye size comparable to the human eye. We found significant cell death within the outer nuclear layer of the retina within 30 hours of injection of ATP into the cat vitreous. Widespread photoreceptor death accounts for our observation of functional and structural degeneration continuing out to 12 weeks in ATP injected eyes. Although the mechanism of ATP induced photoreceptor loss is not well understood, it is possible that direct toxicity via over-activation of $P2X_7$ receptors, which are known to be expressed by photoreceptors, explains the observations[23, 29, 45, 46]. Alternatively, ATP induced effects on the RPE could also induce secondary effects on photoreceptor integrity[47, 48].

Specific to the cat was rapid loss of rod function, followed by a gradual loss of cone function over a 12 week period. Previous characterisation of the effects of ATP on

rodent photoreceptor integrity showed rapid loss of both rod and cone mediated function[24]. It is possible that the distribution of purinergic receptors, and thus the underlying mechanism of vulnerability in rods and cones, is different in cat retina compared to the rat. As ATP is rapidly broken down within the eye by ecto-nucleoside-tri-phosphate-diphosphohydrolases (E-NTPDases)[49] it is likely that continued cone loss after the initial insult is a secondary effect instigated by widespread rod loss as is commonly seen in both human and animal inherited retinal degenerations[50, 51]. A loss of rod function before cone function in our model is ideal as it loosely mimics the course of human RP[52, 53].

In RP, there is a relationship between outer nuclear layer thickness and residual ERG amplitude[54]. Our model also showed a thinning of the outer nuclear layer by 12 weeks post injection, but this rate of loss did not correlate closely to the loss of the ERG. It is possible that the rapid rate of degeneration in our model overwhelms the retina's ability to remove dead and dying cells from the outer nuclear layer and leads to a build-up of non-functional detritus in this layer. Additionally, as OCT only gives a gross representation of each layer and does not account for cell type, our quantification of the outer nuclear layer may include a larger proportion of inflammatory cells that have invaded the retina in response to ATP induced degeneration.

ATP induced inner retinal changes in cat:

436 Although high levels of extracellular ATP primarily affected photoreceptor integrity in
437 the cat retina, some changes in the inner retina were noted. In particular, two weeks
438 following injection with 11 mM ATP, there was a reduction in the amplitude of the
439 oscillatory potentials even in animals with otherwise relatively intact a-wave
440 amplitudes. This runs contrary to previous findings in human patients with RP which
441 showed a relative survival of the OP amplitudes[44] . The OPs are thought to primarily
442 represent the function of inner retinal neurons, especially amacrine cells[39]. OP
443 amplitude is particularly sensitive to ischemia in even small areas of the retina[55], and
444 loss of OPs is evident in all forms of retinal detachment, even after resolution of the
445 condition[56-58]. With this in mind it is possible that the loss of OP amplitudes observed
446 in our model could be attributed to the localised retinal detachments we observed in
447 many of the ATP injected eyes. Alternatively, changes in OP amplitudes may be
448 indicative of a direct effect of ATP on inner retinal neurons, or as a result of the inner
449 retinal swelling we observed in animals 2 weeks after injection.
450
451 Thickness of the inner retina was significantly increased six weeks after injection with
452 11mM ATP, but was restored by 12 weeks. This resembles inner retinal swelling as
453 previously observed from OCTs in human retinal degenerations[59-61]. We propose
454 that increased thickness represents intraretinal oedema in response to ongoing
455 degeneration. This could explain the greater increase in thickness across the area
456 centralis in our model; continued cone degeneration would be the primary contributor
457 to intraretinal oedema at 6 and 12 week time points, and the area centralis has the
458 highest cone density in the cat retina[62]. It seems probable that retinal swelling would
459 not be confined solely to the inner retina in this case, but loss of the outer nuclear

460 layer would mask the increase in thickness from intraretinal oedema in the outer
461 retina when examined by OCT.
462
463 Significantly, our results show that the nerve fibre layer remained intact suggesting
464 that even though photoreceptors and perhaps some minor changes in the inner
465 retina were observed, ganglion cells and their axons remain intact. This is important
466 if this model is to be used in the future for evaluating the success of vision
467 restoration strategies such as retinal prostheses, which require functional ganglion
468 cells.
469
470 ***ATP injection as a model of retinal degeneration*:**
471 The ATP induced model of photoreceptor death in the feline model is potentially
472 suitable for use as an animal model of retinal degeneration. In the cat, ATP induces
473 a loss of outer retinal structure and function within 12 weeks whilst leaving the inner
474 retina relatively intact. Although ATP is not a primary cause of photoreceptor loss in
475 those with inherited retinal degenerations, it has been proposed to exacerbate
476 photoreceptor loss[28, 46]. Moreover, remodelling of the inner retina after photoreceptor
477 degeneration is thought to occur regardless of the initial underlying mechanism[3, 5, 63,
478 64].
479
480 The ATP induced feline model of retinal degeneration has several key advantages
481 over transgenic larger-eyed animal models of degeneration traditionally used in
482 vision research[11, 65]. Logistically, these transgenic animal models tend to be
483 prohibitively expensive to develop and maintain. Often the rate of disease
484 progression is quite slow - for example, the Abyssinian cat model of retinal

485 degeneration still has significant residual ERG at 3-4 years of age[66]. A faster model
486 of degeneration does exist in Persian cats[67], but photoreceptors do not have time to
487 fully develop in this model before the onset of degeneration. Our pharmacological
488 model of degeneration therefore has the advantage of being comparatively cheap,
489 fast acting and readily accessible compared to these other models. Furthermore,
490 unilateral injection of ATP allows for normal sight in the fellow eye, which can then
491 act as an internal control and reduce housing and ethics considerations as the
492 affected animal retains functional vision.
493
494 An ATP induced model of feline degeneration however has several limitations. As a
495 pharmacological model of degeneration, the disease process does not model human
496 disease as closely as models where genetic manipulations induce photoreceptor
497 death. In addition, we observed multiple focal retinal detachments in some cats
498 within 2 weeks of intravitreal injection of ATP. Unfortunately, these retinal
499 detachments tended to worsen at high concentrations where the degenerative
500 process was otherwise more reliable. These detachments were visually similar to
501 those described in a recent study of OCT in RD10 mouse[68]. It may be that the acute
502 rate of degeneration in our model interferes with and overwhelms fluid transfer at the
503 retinal pigment epithelium (RPE), leading to retinal elevation and eventually
504 detachment. It is also possible that ATP has a direct effect on fluid transfer at the
505 RPE[48].
506
507 In conclusion, this study aimed to develop and characterise an ATP-induced model
508 of retinal degeneration in the cat retina. We examined retinal function and structure
509 using a combination of ERG and OCT imaging to determine a dose response and

510 time course of degeneration. All concentrations of ATP tested caused widespread
511 photoreceptor death and loss of retinal function within 2 weeks of injection. In
512 particular, intravitreal injection with 11mM ATP lead to a rapid loss of rod and a
513 gradual loss of cone function over a 12 week period. Outer retinal thickness
514 continued to reduce throughout the 12 week period. The inner retina showed some
515 evidence of intraretinal swelling, but otherwise remained intact. This ATP-induced
516 feline model of retinal degeneration provides a new animal model for research into
517 vision restoration.
518
519

1. Taylor HR, Keeffe JE, Vu HTV, et al. Vision loss in Australia. *Medical Journal of Australia* 2005;182:565-568.
2. Fariss RN, Li ZY, Milam AH. Abnormalities in rod photoreceptors, amacrine cells, and horizontal cells in human retinas with retinitis pigmentosa. *American Journal of Ophthalmology* 2000;129:215-223.
3. Jones BW, Watt CB, Frederick JM, et al. Retinal remodeling triggered by photoreceptor degenerations. *Journal of Comparative Neurology* 2003;464:1-16.
4. Kalloniatis M, Fletcher EL. Retinitis pigmentosa: Understanding the clinical presentation, mechanisms and treatment options. *Clinical and Experimental Optometry* 2004;87:65-80.
5. Marc RE, Jones BW, Watt CB, Strettoi E. Neural remodeling in retinal degeneration. *Progress in Retinal and Eye Research* 2003;22:607-655.
6. Strettoi E, Pignatelli V, Rossi C, Porciatti V, Falsini B. Remodeling of second-order neurons in the retina of rd/rd mutant mice. *Vision Research* 2003;43:867-877.
7. O'Brien EE, Greferath U, Vessey KA, Jobling AI, Fletcher EL. Electronic restoration of vision in those with photoreceptor degenerations. *Clinical and Experimental Optometry* 2012;95:473-483.
8. Seiler MJ, Aramant RB. Cell replacement and visual restoration by retinal sheet transplants. *Progress in Retinal and Eye Research* 2012;31:661-687.
9. Dahlmann-Noor A, Vijay S, Jayaram H, Limb A, Khaw PT. Current approaches and future prospects for stem cell rescue and regeneration of the retina and optic nerve. *Canadian Journal of Ophthalmology* 2010;45:333-341.
10. Singh MS, Issa PC, Butler R, et al. Reversal of end-stage retinal degeneration and restoration of visual function by photoreceptor transplantation. *Proceedings of the National Academy of Sciences of the United States of America* 2013;110:1101-1106.
11. Bertschinger DR, Beknazar E, Simonutti M, et al. A review of in vivo animal studies in retinal prosthesis research. *Graefe's Archive for Clinical and Experimental Ophthalmology* 2008;246:1505-1517.
12. Nayagam DAX, Williams RA, Allen PJ, et al. Chronic electrical stimulation with a suprachoroidal retinal prosthesis: A preclinical safety and efficacy study. *PLoS ONE* 2014;9.
13. Narfstrom K. Progressive retinal atrophy in the Abyssinian cat. Clinical characteristics. *Investigative Ophthalmology and Visual Science* 1985;26:193-200.
14. Narfstrom K, Nilsson SE. Progressive retinal atrophy in the Abyssinian cat. Electron microscopy. *Investigative Ophthalmology and Visual Science* 1986;27:1569-1576.
15. Wrigstad A, Nilsson SEG, Narfstrom K. Ultrastructural changes of the retina and the retinal pigment epithelium in briard dogs with hereditary congenital night blindness and partial day blindness. *Experimental Eye Research* 1992;55:805-818.
16. Narfstrom K, Wrigstad A, Nilsson SEG. The Briard dog: A new animal model of congenital stationary night blindness. *British Journal of Ophthalmology* 1989;73:750-756.
17. Sargan DR, Clements PJ, Sohal A, Gregory CY, Bhattacharya SS, Petersen-Jones SM. Progressive retinal atrophy: a model for retinitis pigmentosa in companion animals. *Gene therapy* 1994;1 Suppl 1.
18. Yokoyama D, MacHida S, Kondo M, Terasaki H, Nishimura T, Kurosaka D. Pharmacological dissection of multifocal electroretinograms of rabbits with Pro347Leu rhodopsin mutation. *Japanese Journal of Ophthalmology* 2010;54:458-466.
19. Li ZY, Wong F, Chang JH, et al. Rhodopsin transgenic pigs as a model for human retinitis pigmentosa. *Investigative Ophthalmology and Visual Science* 1998;39:808-819.
20. Jones BW, Kondo M, Terasaki H, et al. Retinal remodeling in the Tg P347L rabbit, a large-eye model of retinal degeneration. *Journal of Comparative Neurology* 2011;519:2713-2733.
21. Kiuchi K, Yoshizawa K, Shikata N, Moriguchi K, Tsubura A. Morphologic characteristics of retinal degeneration induced by sodium iodate in mice. *Current Eye Research* 2002;25:373-379.

22. Tsubura A, Lai YC, Miki H, et al. Animal models of N-methyl-N-nitrosourea-induced mammary cancer and retinal degeneration with special emphasis on therapeutic trials. *In Vivo* 2011;25:11-22.
23. Puthussery T, Fletcher E. Extracellular ATP induces retinal photoreceptor apoptosis through activation of purinoceptors in rodents. *Journal of Comparative Neurology* 2009;513:430-440.
24. Vessey KA, Greferath U, Aplin FP, et al. Adenosine triphosphate-induced photoreceptor death and retinal remodeling in rats. *Journal of Comparative Neurology* 2014.
25. Köles L, Leichsenring A, Rubini P, Illes P. P2 Receptor Signaling in Neurons and Glial Cells of the Central Nervous System. 2011:441-493.
26. Wang X, Arcuino G, Takano T, et al. P2X7 receptor inhibition improves recovery after spinal cord injury. *Nature Medicine* 2004;10:821-827.
27. Peng W, Cotrina ML, Han X, et al. Systemic administration of an antagonist of the ATP-sensitive receptor P2X7 improves recovery after spinal cord injury. *Proceedings of the National Academy of Sciences of the United States of America* 2009;106:12489-12493.
28. Fletcher EL. Mechanisms of photoreceptor death during retinal degeneration. *Optometry and Vision Science* 2010;87:269-275.
29. Puthussery T, Fletcher EL. Synaptic Localization of P2X7 Receptors in the Rat Retina. *Journal of Comparative Neurology* 2004;472:13-23.
30. Puthussery T, Fletcher EL. P2X2 receptors on ganglion and amacrine cells in cone pathways of the rat retina. *Journal of Comparative Neurology* 2006;496:595-609.
31. Hu H, Lu W, Zhang M, et al. Stimulation of the P2X7 receptor kills rat retinal ganglion cells in vivo. *Experimental Eye Research* 2010;91:425-432.
32. Zhang X, Zhang M, Laties AM, Mitchell CH. Balance of purines may determine life or death of retinal ganglion cells as A3 adenosine receptors prevent loss following P2X7 receptor stimulation. *Journal of Neurochemistry* 2006;98:566-575.
33. Zhang X, Zhang M, Laties AM, Mitchell CH. Stimulation of P2X7 Receptors Elevates Ca2+ and Kills Retinal Ganglion Cells. *Investigative Ophthalmology & Visual Science* 2005;46:2183-2191.
34. Vakkur GJ, Bishop PO. The schematic eye in the cat. *Vision Research* 1963;3:357-360,IN319,361-364,IN321-IN323,365,IN325,366-381.
35. Gekeler F, Szurman P, Grisanti S, et al. Compound subretinal prostheses with extra-ocular parts designed for human trials: Successful long-term implantation in pigs. *Graefe's Archive for Clinical and Experimental Ophthalmology* 2007;245:230-241.
36. Güven D, Weiland JD, Fujii G, et al. Long-term stimulation by active epiretinal implants in normal and RCD1 dogs. *Journal of Neural Engineering* 2005;2:S65-S73.
37. Terasawa Y, Tashiro H, Nakano Y, Osawa K, Ozawa M. Safety assessment of semichronic suprachoroidal electrical stimulation to rabbit retina. *Proceedings of the Annual International Conference of the IEEE Engineering in Medicine and Biology Society, EMBS* 2013;3567-3570.
38. Villalobos J, Nayagam DA, Allen PJ, et al. A wide-field suprachoroidal retinal prosthesis is stable and well tolerated following chronic implantation. *Investigative ophthalmology & visual science* 2013;54:3751-3762.
39. Weymouth AE, Vingrys AJ. Rodent electroretinography: Methods for extraction and interpretation of rod and cone responses. *Progress in Retinal and Eye Research* 2008;27:1-44.
40. Jobling AI, Vessey KA, Waugh M, Mills SA, Fletcher EL. A naturally occurring mouse model of achromatopsia: Characterization of the mutation in cone transducin and subsequent retinal phenotype. *Investigative Ophthalmology and Visual Science* 2013;54:3350-3359.
41. Komaromy AM, Smith PJ, Brooks DE. Electroretinography in dogs and cats. Part I. Retinal morphology and physiology. *Compendium on Continuing Education for the Practicing Veterinarian* 1998;20:343-350.
42. Robson JG, Frishman LJ. Dissecting the dark-adapted electroretinogram. *Documenta Ophthalmologica* 1998;95:187-215.
43. Vaegan, Millar TJ. Effect of kainic acid and NMDA on the pattern electroretinogram, the scotopic threshold response, the oscillatory potentials and the electroretinogram in the urethane anaesthetized cat. *Vision Research* 1994;34:1111-1125.

624 44. Ikenoya K, Kondo M, Piao C-H, Kachi S, Miyake Y, Terasaki H. Preservation of Macular
625 Oscillatory Potentials in Eyes of Patients with Retinitis Pigmentosa and Normal Visual Acuity.
626 *Investigative Ophthalmology & Visual Science* 2007;48:3312-3317.
627 45. Puthussery T, Yee P, Vingrys AJ, Fletcher EL. Evidence for the involvement of purinergic
628 P2X7 receptors in outer retinal processing. *European Journal of Neuroscience* 2006;24:7-19.
629 46. Ward MM, Puthussery T, Vessey KA, Fletcher EL. The role of purinergic receptors in retinal
630 function and disease. *Advances in Experimental Medicine and Biology* 2010;664:385-391.
631 47. Mitchell CH. Release of ATP by a human retinal pigment epithelial cell line: Potential for
632 autocrine stimulation through subretinal space. *Journal of Physiology* 2001;534:193-202.
633 48. Mitchell CH, Reigada D. Purinergic signalling in the subretinal space: A role in the
634 communication between the retina and the RPE. *Purinergic Signalling* 2008;4:101-107.
635 49. Ricatti MJ, Alfie LD, Lavoie ÉG, Sévigny J, Schwarzbaum PJ, Faillace MP.
636 Immunocytochemical localization of NTPDases1 and 2 in the neural retina of mouse and zebrafish.
637 *Synapse* 2009;63:291-307.
638 50. García-Ayuso D, Ortín-Martínez A, Jiménez-López M, et al. Changes in the photoreceptor
639 mosaic of P23H-1 rats during retinal degeneration: Implications for rod-cone dependent survival.
640 *Investigative Ophthalmology and Visual Science* 2013;54:5888-5900.
641 51. Bovolenta P, Cisneros E. Retinitis pigmentosa: Cone photoreceptors starving to death. *Nature*
642 *Neuroscience* 2009;12:5-6.
643 52. Fasiuddin A. Inherited retinal degenerations. *International Ophthalmology Clinics*
644 2010;50:45-56.
645 53. Milam AH, Li ZY, Fariss RN. Histopathology of the human retina in retinitis pigmentosa.
646 *Progress in Retinal and Eye Research* 1998;17:175-205.
647 54. Cideciyan AV, Aleman TS, Boye SL, et al. Human gene therapy for RPE65 isomerase
648 deficiency activates the retinoid cycle of vision but with slow rod kinetics. *Proceedings of the*
649 *National Academy of Sciences* 2008.
650 55. Speros P, Price J. Oscillatory potentials. History, techniques and potential use in the
651 evaluation of disturbances of retinal circulation. *Survey of Ophthalmology* 1981;25:237-252.
652 56. Kim IT, Ha SM, Yoon KC. Electroretinographic studies in rhegmatogenous retinal
653 detachment before and after reattachment surgery. *Korean journal of ophthalmology : KJO*
654 2001;15:118-127.
655 57. Gong Y, Wu X, Sun X, Zhang X, Zhu P. Electroretinogram changes after scleral buckling
656 surgery of retinal detachment. *Documenta Ophthalmologica* 2008;117:103-109.
657 58. Lewis GP, Charteris DG, Sethi CS, Fisher SK. Animal models of retinal detachment and
658 reattachment: Identifying cellular events that may affect visual recovery. *Eye* 2002;16:375-387.
659 59. Aleman TS, Cideciyan AV, Sumaroka A, et al. Retinal laminar architecture in human retinitis
660 pigmentosa caused by Rhodopsin gene mutations. *Investigative Ophthalmology and Visual Science*
661 2008;49:1580-1591.
662 60. Zhang Y, Huang H, Wei S, et al. Characterization of retinal nerve fiber layer thickness
663 changes associated with leber's hereditary optic neuropathy by optical coherence tomography.
664 *Experimental and Therapeutic Medicine* 2014;7:483-487.
665 61. Hood DC, Lazow MA, Locke KG, Greenstein VC, Birch DG. The transition zone between
666 healthy and diseased retina in patients with retinitis pigmentosa. *Investigative Ophthalmology and*
667 *Visual Science* 2011;52:101-108.
668 62. Steinberg RH, Reid M, Lacy PL. The distribution of rods and cones in the retina of the cat
669 (Felis domesticus). *The Journal of Comparative Neurology* 1973;148:229-248.
670 63. Jones BW, Watt CB, Marc RE. Retinal remodelling. *Clinical and Experimental Optometry*
671 2005;88:282-291.
672 64. Marc RE, Jones BW, Watt CB, Vazquez-Chona F, Vaughan DK, Organisciak DT. Extreme
673 retinal remodeling triggered by light damage: Implications for age related macular degeneration.
674 *Molecular Vision* 2008;14:782-806.
675 65. Fletcher EL, Jobling AI, Vessey KA, Luu C, Guymer RH, Baird PN. Animal models of
676 retinal disease. *Progress in Molecular Biology and Translational Science*; 2011:211-286.

66. Kang Derwent JJ, Padnick-Silver L, McRipley M, Giuliano E, Linsenmeier RA, Narfström K. The electroretinogram components in Abyssinian cats with hereditary retinal degeneration. *Investigative Ophthalmology and Visual Science* 2006;47:3673-3682.
67. Rah H, Maggs DJ, Blankenship TN, Narfstrom K, Lyons LA. Early-onset, autosomal recessive, progressive retinal atrophy in Persian cats. *Investigative Ophthalmology and Visual Science* 2005;46:1742-1747.
68. Pennesi ME, Michaels KV, Magee SS, et al. Long-term characterization of retinal degeneration in rd1 and rd10 mice using spectral domain optical coherence tomography. *Investigative Ophthalmology and Visual Science* 2012;53:4644-4656.

Figure Legends:

Figure 1. OCT acquisition and analysis. Representative infrared reflectance fundus images in a control animal showing location of OCT scans across the temporal retina and area centralis (A), Nasal retina and around the optic nerve (B). OCT section thickness was separated into total retina, inner retina and outer retina in linear scans (C) or total retina, retinal nerve fibre layer (RNFL) and retina excluding the RNFL (GCL+) in the circular scan around the optic nerve (D). Scale bar, 200 μm. RNFL, retinal nerve fibre layer; GCL, ganglion cell layer; IPL, inner plexiform layer, INL, inner nuclear layer; OPL, outer plexiform layer; ONL, outer nuclear layer; IS/OS, inner and outer segments; RPE, retinal pigment epithelium;

Figure 2. ATP induces photoreceptor death at 30 hours in cat retina. Sections of retinae labelled for apoptosis (TUNEL) after 30 hours in a saline injected eye (A) and in central (B) and peripheral (C) retina of an ATP injected eye. In each condition, the number of TUNEL positive photoreceptors were counted and quantified per mm (D) and as a percentage of total photoreceptors per mm (E). There was a significant difference between saline (0.01 cells/mm, data not shown) and ATP injected eyes (1-way ANOVA; $P < 0.01$; $n = 4$) but no significant difference between location in ATP

705 injected eyes (1-way ANOVA; P > 0.05; n = 4) Scale bar, 200 μm. Abbreviations: as
706 in Figure 1. Asterisks (*) indicate significant difference P < 0.05.
707
708 **Figure 3. ATP induces dose-dependent loss of retinal function at 2 weeks.** Full-
709 field ERG combined rod-cone maximal responses (10 cd.s/m^2) were used to assess
710 retinal function after 2 weeks in untreated, saline injected and 11, 22 and 55mM ATP
711 injected eyes. (A) representative maximal ERG response waveforms of control and
712 three ATP injection concentrations. Maximal ERG a-wave (B) and b-wave (C)
713 amplitudes were assessed in each condition. (D) representative oscillatory potential
714 waveforms in control and three ATP injection concentrations. Summed OP1-4
715 amplitude (E) was assessed in each condition. There was a significant decrease in
716 a-wave and b-wave amplitude after 2 weeks in eyes injected with 11, 22 and 55mM
717 ATP (Kruskal-Wallis; P < 0.05, n = 3 for 22mM injected eyes; 4 for 55mM injected
718 eyes; 8 for control, sham and 11mM injected eyes) but not between control and
719 sham injected eyes (Kruskal-Wallis; P > 0.05, n = 8). Asterisks (*) indicate significant
720 difference P < 0.05.
721
722 **Figure 4. ATP induces dose-dependent retinal thinning and detachment at 2**
723 **weeks.** Representative temporal linear OCT sections in control eyes (A) and 2
724 weeks after injection with 11 mM (B), 22 mM (C) and 55 mM (D) ATP. Total retinal
725 thickness was assessed in control, sham injected and ATP injected eyes at each
726 concentration (E). White arrows (B-C) indicate retinal detachments. The retinal
727 thickness in eyes injected with 55mM ATP was significantly reduced compared to
728 control, sham injected and 11 mM injected eyes (Kruskal-Wallis; P < 0.05; n = 3 for
729 22mM injected eyes; 4 for 55mM injected eyes; 8 for control, sham and 11mM

730 injected eyes). There were no other significant differences (Kruskal-Wallis; P > 0.05;
731 n = 3-8). Scale bar, 100 μm. Asterisks (*) indicate significant difference P < 0.05.
732
733 **Figure 5. Rod and cone function is reduced within 12 weeks after injection with**
734 **11 mM ATP.** Twin-flash full-field ERGs (10 cd.s/m^2) were used to isolate rod and
735 cone function in control eyes and at 2, 6 and 12 weeks after injection with 11mM
736 ATP. (A) representative waveforms of the isolated rod response in controls and at
737 three time points post ATP injection. Rod a-wave (B) and b-wave (C) amplitudes
738 were assessed at each time point. (D) representative waveforms of the cone
739 response in control and at three time points post ATP injection. Cone a-wave (E) and
740 b-wave (F) amplitudes were assessed at each time point. Rod a-wave and b-wave
741 amplitudes were significantly reduced by 2 weeks (1-way ANOVA; P < 0.05; n= 8-
742 13). Cone a-wave and b-wave amplitudes were significantly reduced by 12 weeks
743 and 6 weeks respectively (1-way ANOVA; P < 0.05; n= 8-13). Asterisks (*) indicate
744 significant difference P < 0.05.
745
746 **Figure 6. Oscillatory potential amplitude reduction may indicate some inner**
747 **retinal degeneration.** Oscillatory potential amplitudes were digitally subtracted from
748 mixed b-wave output and analysed separately. (A) representative OP waveforms in
749 control eyes and at 2, 6 and 12 weeks after injection with 11 mM ATP. Summed
750 OP1-4 amplitudes were assessed at each time point (B). Mixed a-wave amplitude
751 was correlated to summed OP amplitude (C) and mixed b-wave amplitude (D) in
752 control eyes and at 2 weeks after injection with 11mM ATP. Summed OP amplitude
753 had significantly decreased by 2 weeks (1-way ANOVA; P < 0.05; n= 8-13). The
754 amplitude of the mixed a-wave is correlated with the amplitude of both summed OP

amplitude and mixed b-wave amplitude (Deming regression; $P < 0.01$; n = 8-13). Two weeks after ATP injection, the slope of the summed OP and a-wave correlation was significantly different compared to controls (Deming regression; $P < 0.05$; n = 8-13), indicating a greater decrease in OP amplitude compared to loss of the a-wave. The slope of the b-wave and a-wave correlation was not significantly different at two weeks after ATP injection (Deming regression; $P > 0.05$; n = 8-13). Asterisks (*) indicate significant difference $P < 0.05$.

Figure 7. Representative OCT sections. Representative OCT sections in controls and at 2, 6 and 12 weeks post-injection across the temporal retina (A), area centralis (B), nasal retina (C) and around the optic nerve (D). White arrows indicate focal retinal detachments. White asterisks indicate focal hyper-reflective loci in the vitreous. Scale bar, 200 μm.

Figure 8. Reduction in retinal thickness by eccentricity. (A-C) Mean total retinal thickness (A), outer retinal thickness (B) and inner retina thickness (C) in the temporal retina by distance from the optic nerve in controls and at 2, 6 and 12 weeks following ATP injection. (D-F) Mean total retinal thickness (D), retinal nerve fibre layer thickness (E) and thickness of the retina excluding the RNFL (F) around the optic nerve by orientation from vertical in controls and at 2, 6 and 12 weeks following ATP injection. Grey area = 95% confidence intervals for control retina.

Figure 9. Reduction of OCT retinal thickness is confined to the outer retina. (A-C) Analysis of total, outer, and inner retinal thicknesses in controls and at 2, 6 and 12 weeks post-injection across the temporal retina (A), Area centralis (B) and nasal

780 retina (C). (D) Analysis of total retinal thickness, retinal nerve fibre layer thickness
781 and thickness of the retina excluding the RNFL in controls at 2, 6 and 12 weeks post-
782 injection around the optic nerve. Across the temporal retina, area centralis and nasal
783 retina, total and outer retinal thickness was significantly reduced by 12 weeks
784 (Kruskal-Wallis; $P < 0.05$; $n = 8$). At temporal and nasal locations, inner retinal
785 thickness was significantly increased by 6 weeks (Kruskal-Wallis; $P < 0.05$; $n = 6$-8).
786 By 12 weeks, inner retinal thickness was no longer different compared to controls
787 (Kruskal-Wallis; $P > 0.05$; $n = 6$-8). Across the area centralis, inner retinal thickness
788 remained significantly increased from 2 to 12 weeks compared to controls (Kruskal-
789 Wallis; $P < 0.05$; $n = 8$). Across the optic nerve, total thickness and thickness from
790 the ganglion cell layer were significantly decreased at 12 weeks from controls
791 (Kruskal-Wallis; $P < 0.05$; $n = 8$). Retinal nerve fibre layer thickness was not
792 significantly different from controls at any time point (Kruskal-Wallis; $P > 0.05$; $n = 6$-
793 8). Asterisks (*) indicate significant difference $P < 0.05$.
794

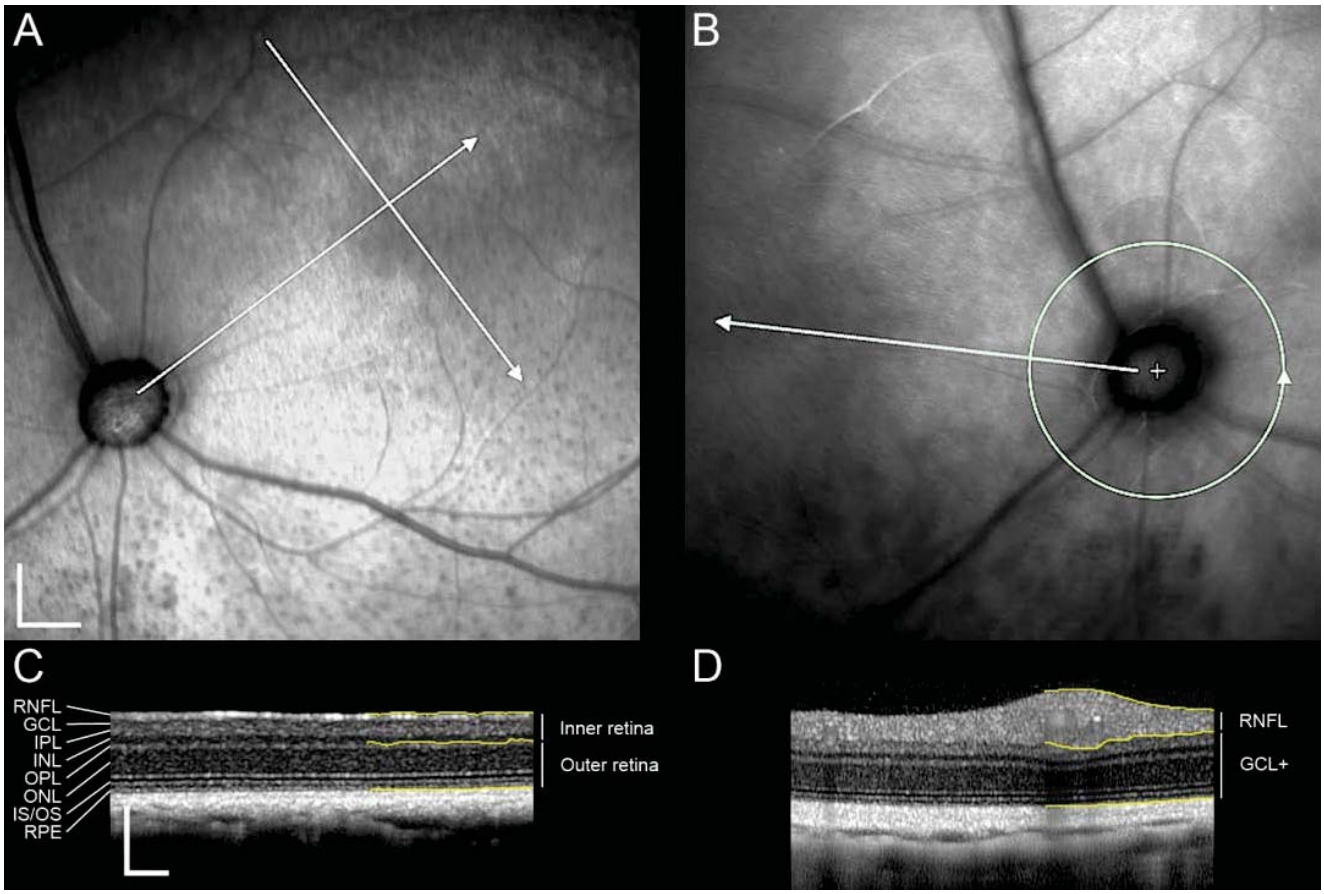
A
B
C
RNFL
GCL
IPL
INL
OPL
ONL
IS/OS
RPE
Inner retina
Outer retina
D
RNFL
GCL+

Figure 1

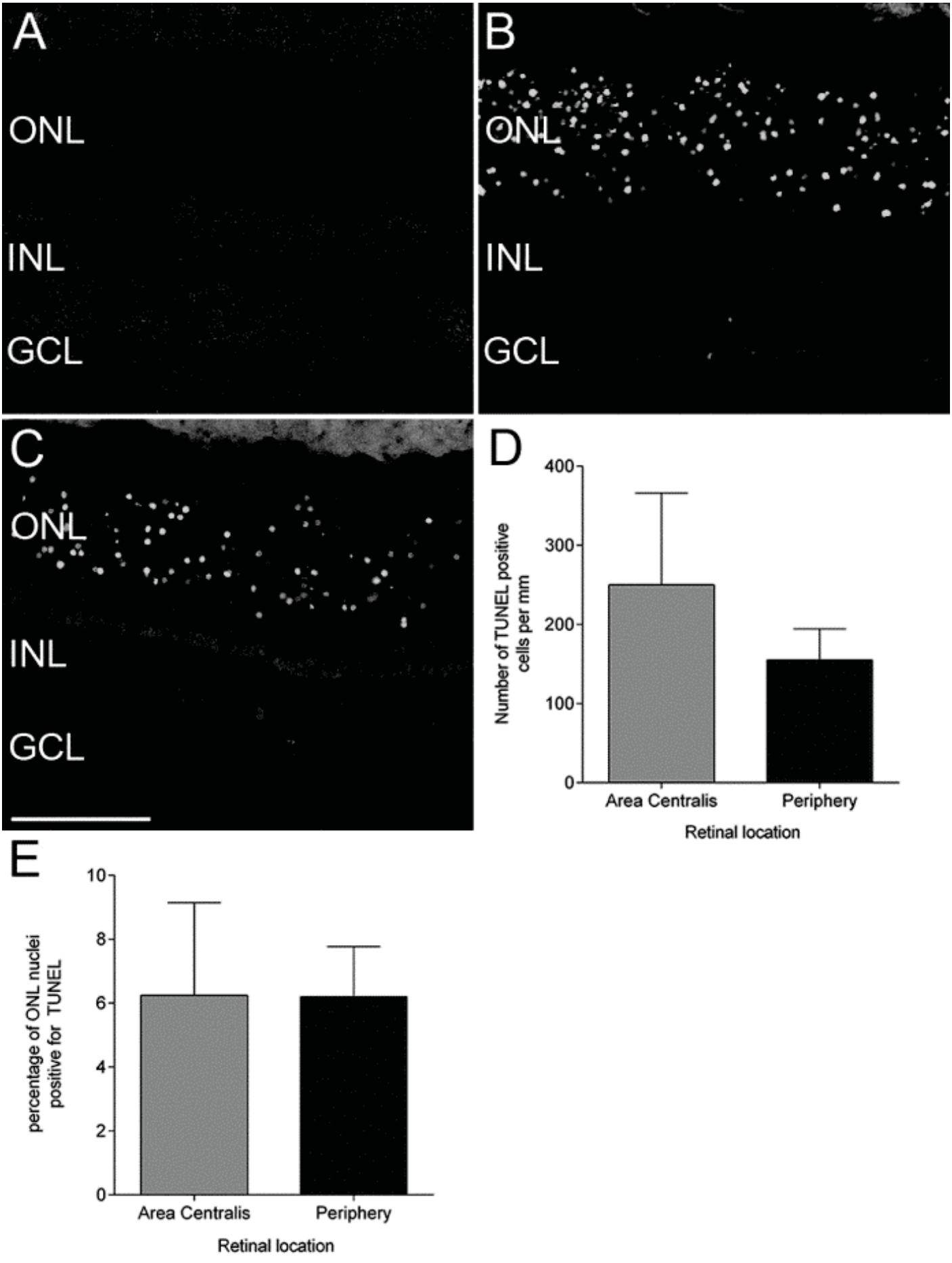
A
ONL
INL
GCL
B
ONL
INL
GCL
C
ONL
INL
GCL
D
Number of TUNEL positive cells per mm
400
300
200
100
0
Area Centralis
Periphery
Retinal location
E
percentage of ONL nuclei positive for TUNEL
10
8
6
4
2
0
Area Centralis
Periphery
Retinal location

Figure 2

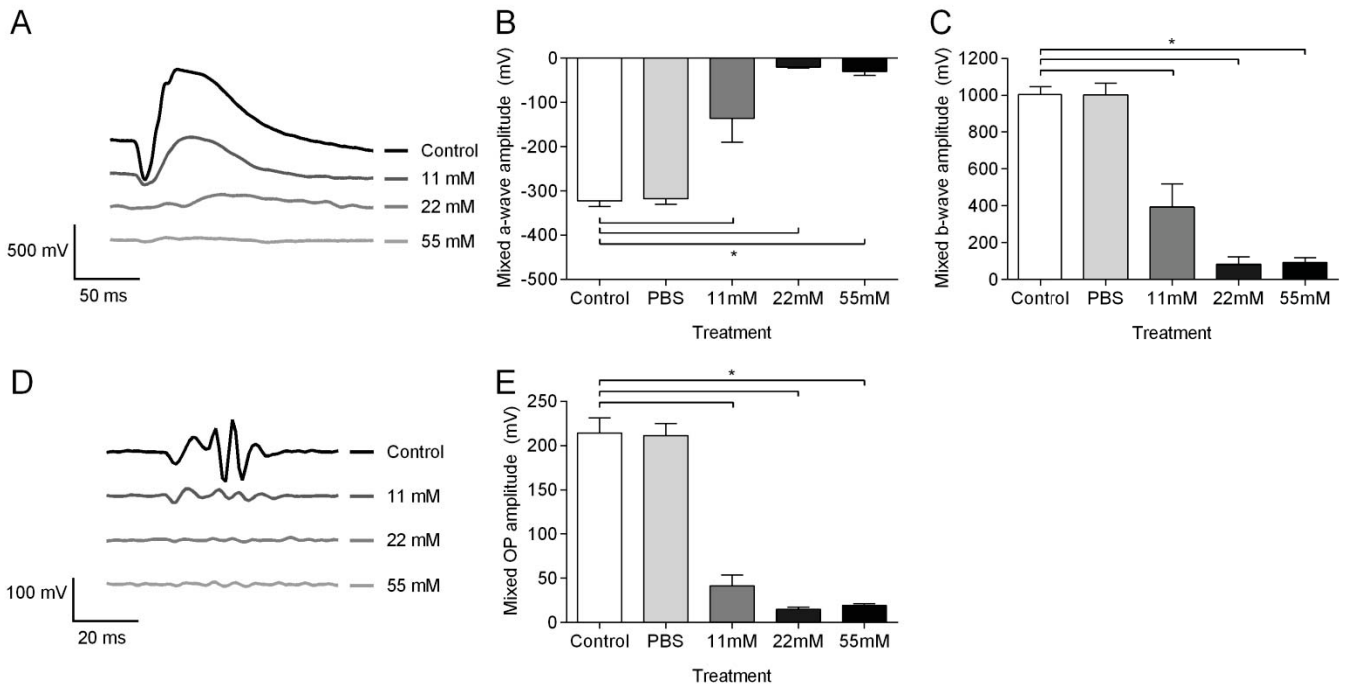
A
Control
11 mM
22 mM
55 mM
500 mV
50 ms
B
Mixed a-wave amplitude (mV)
0
-100
-200
-300
-400
-500
Control
PBS
11mM
22mM
55mM
Treatment
*
C
Mixed b-wave amplitude (mV)
1200
1000
800
600
400
200
0
Control
PBS
11mM
22mM
55mM
Treatment
*
D
Control
11 mM
22 mM
55 mM
100 mV
20 ms
E
Mixed OP amplitude (mV)
250
200
150
100
50
0
Control
PBS
11mM
22mM
55mM
Treatment
*

Figure 3

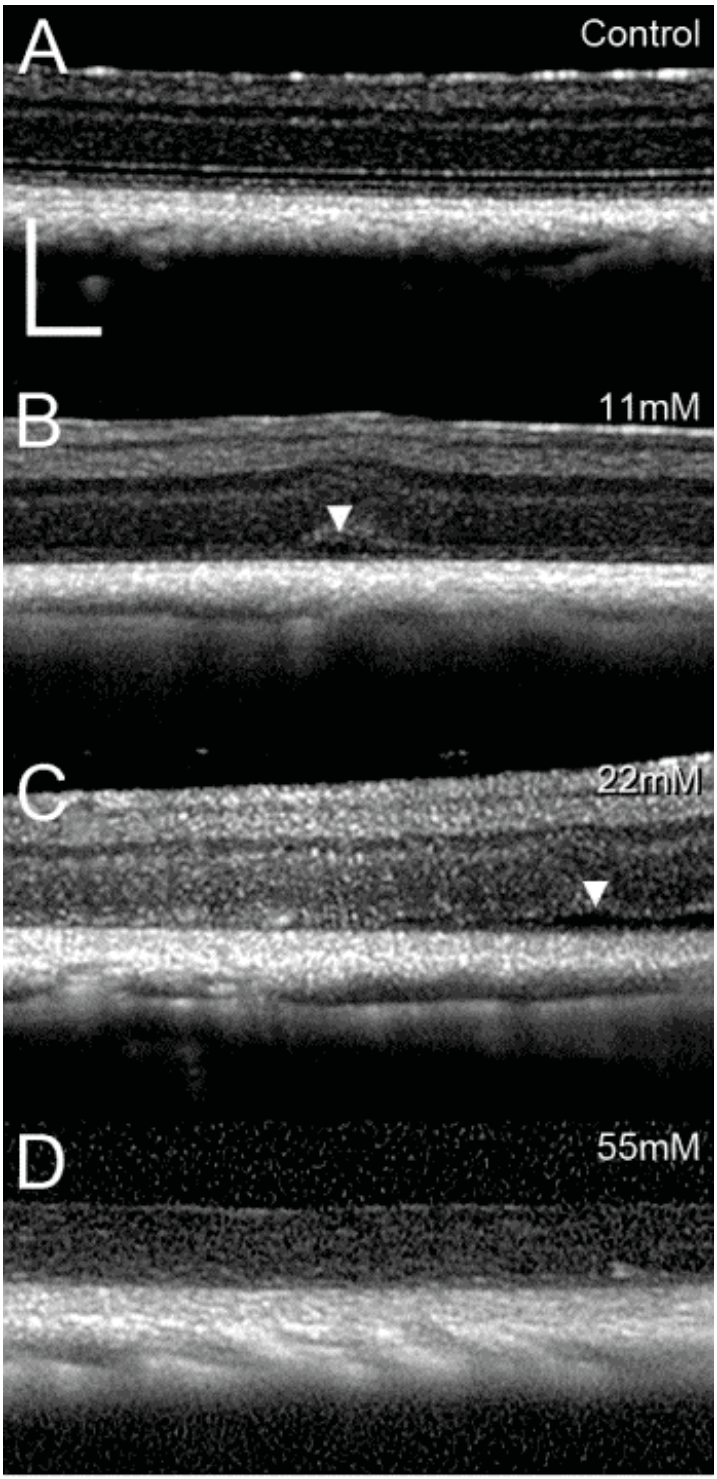
A
Control
L
B
11mM
C
22mM
D
55mM

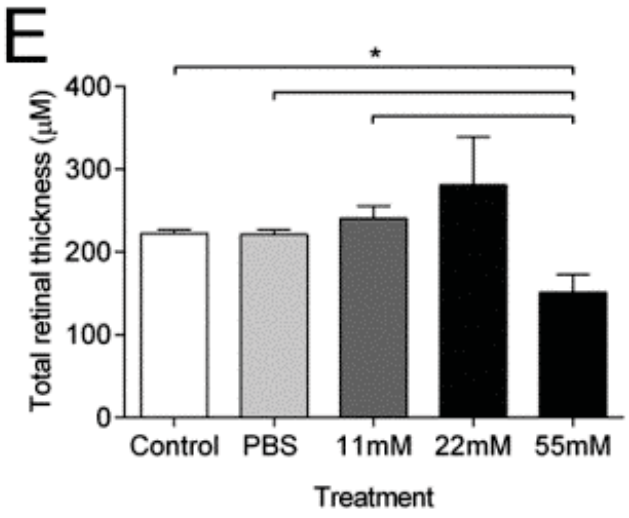
E
*
Total retinal thickness (μM)
400
300
200
100
0
Control
PBS
11mM
22mM
55mM
Treatment

Figure 4

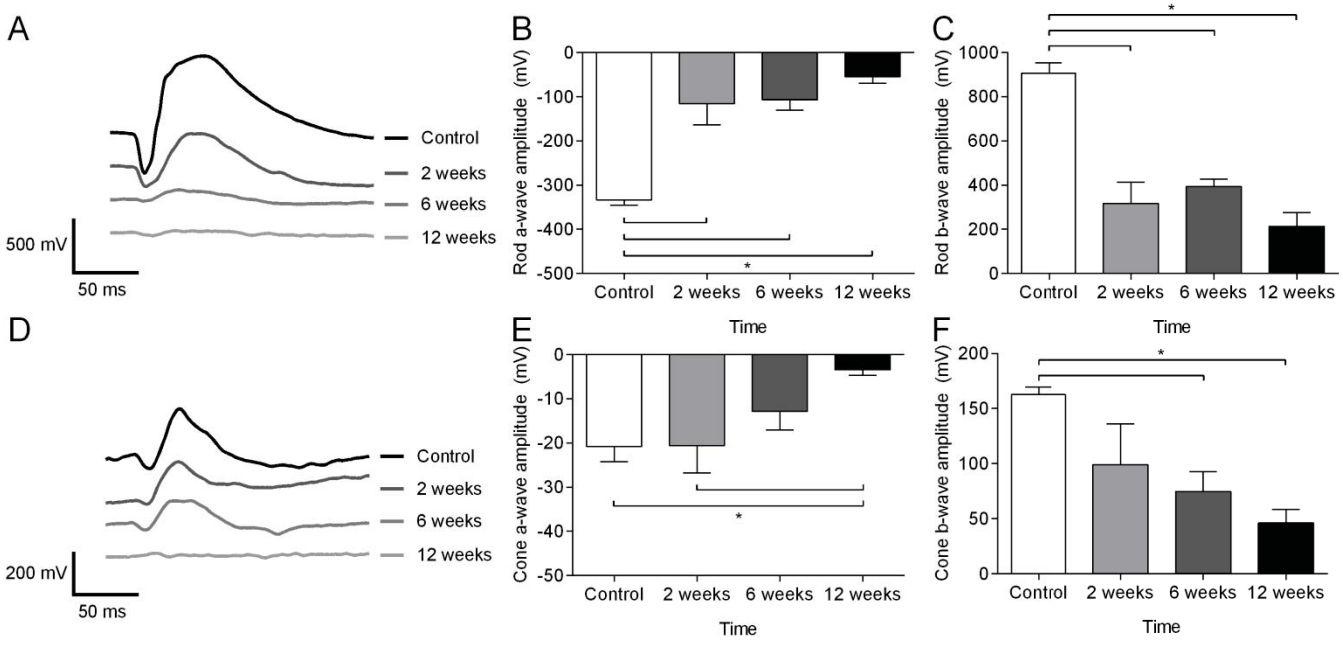
A
Control
2 weeks
6 weeks
12 weeks
500 mV
50 ms
B
Rod a-wave amplitude (mV)
0
-100
-200
-300
-400
-500
*
Control
2 weeks
6 weeks
12 weeks
Time
C
Rod b-wave amplitude (mV)
1000
800
600
400
200
0
*
Control
2 weeks
6 weeks
12 weeks
Time
D
Control
2 weeks
6 weeks
12 weeks
200 mV
50 ms
E
Cone a-wave amplitude (mV)
0
-10
-20
-30
-40
-50
*
Control
2 weeks
6 weeks
12 weeks
Time
F
Cone b-wave amplitude (mV)
200
150
100
50
0
*
Control
2 weeks
6 weeks
12 weeks
Time

Figure5

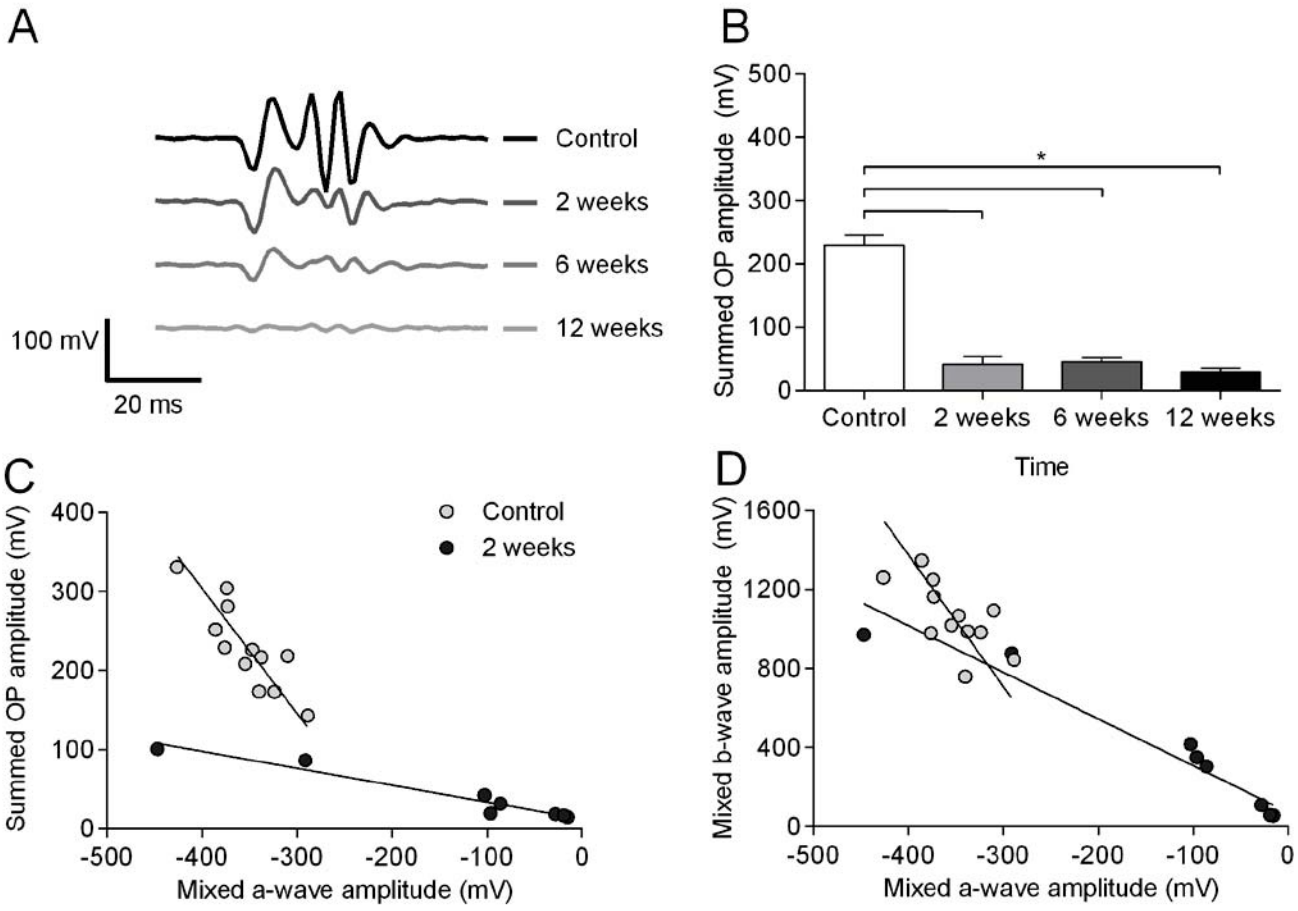
A
Control
2 weeks
6 weeks
12 weeks
100 mV
20 ms
B
Summed OP amplitude (mV)
500
400
300
200
100
0
*
Control
2 weeks
6 weeks
12 weeks
Time
C
Summed OP amplitude (mV)
400
300
200
100
0
Control
2 weeks
-500
-400
-300
-200
-100
0
Mixed a-wave amplitude (mV)
D
Mixed b-wave amplitude (mV)
1600
1200
800
400
0
-500
-400
-300
-200
-100
0
Mixed a-wave amplitude (mV)

Figure 6

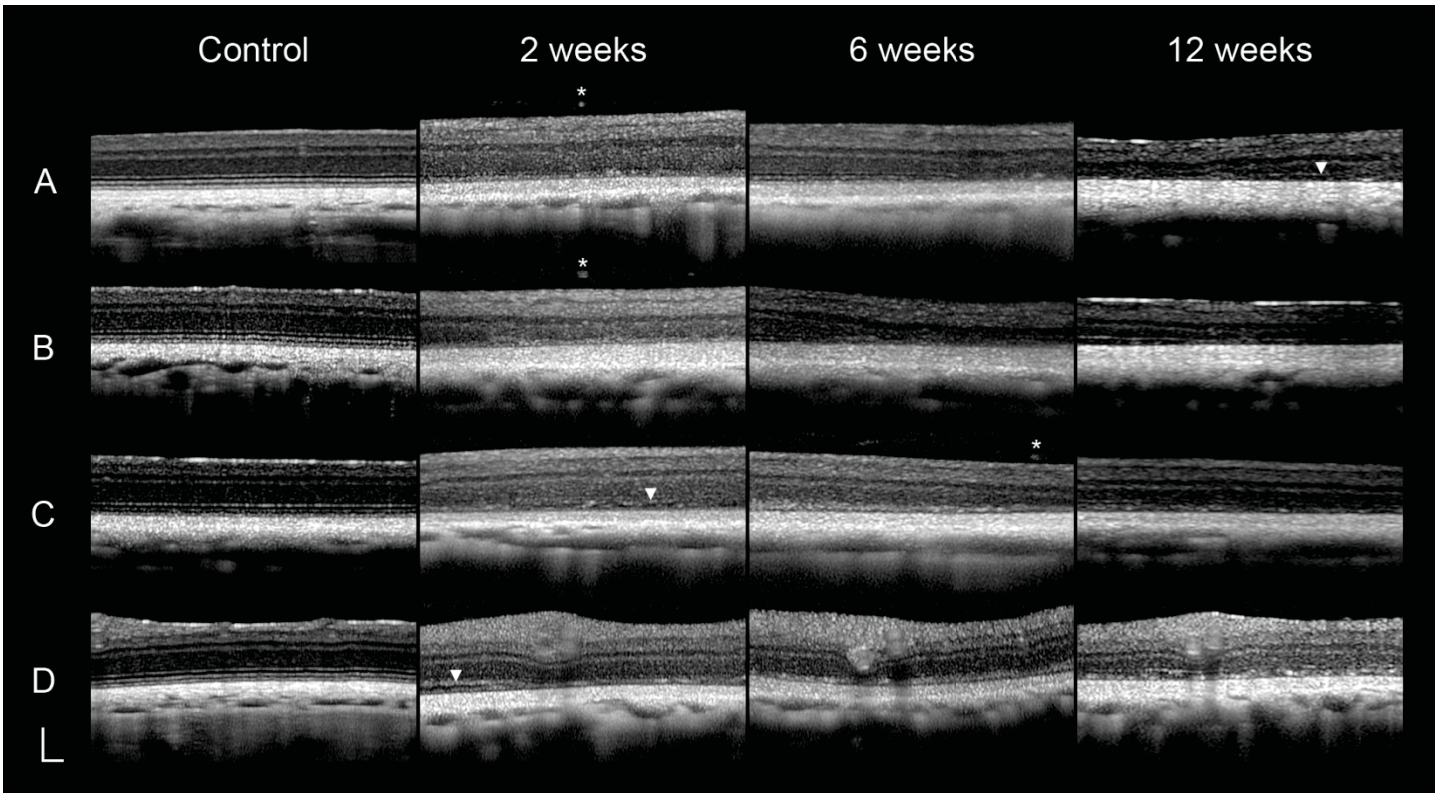

Figure 7

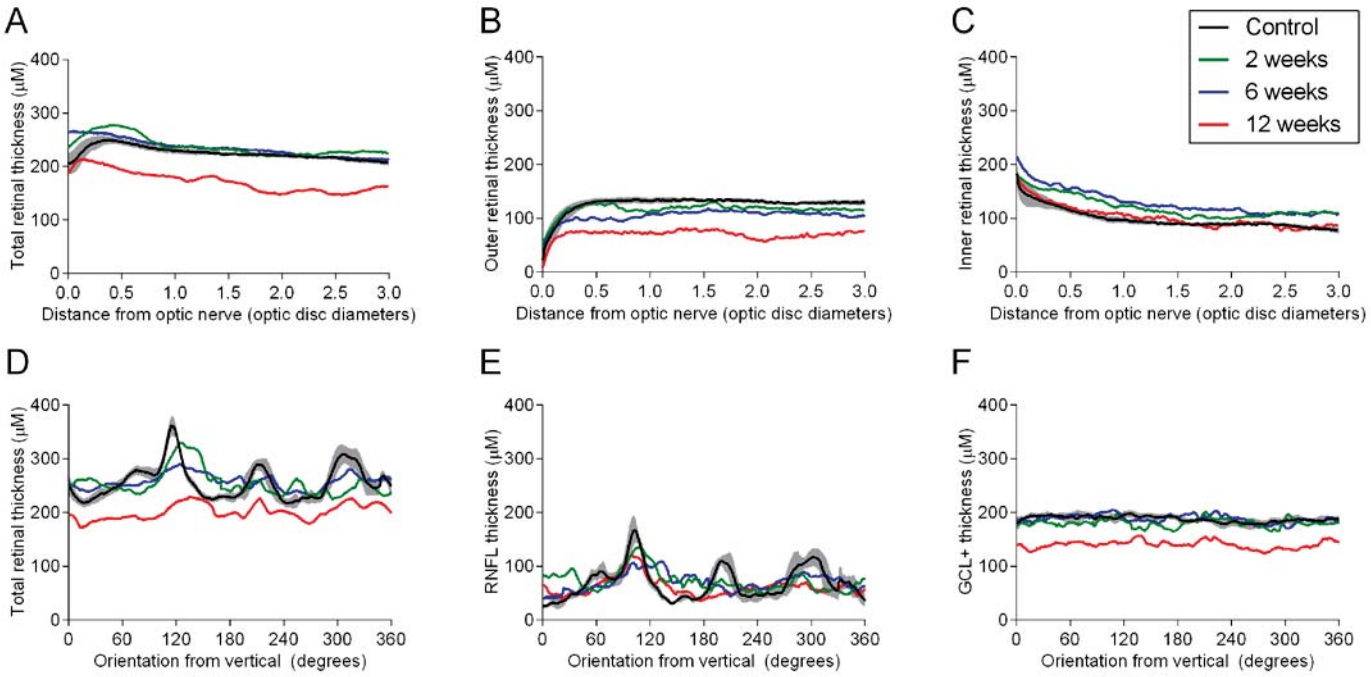
A
B
C
D
E
F
Control
2 weeks
6 weeks
12 weeks
Total retinal thickness (μM)
Outer retinal thickness (μM)
Inner retinal thickness (μM)
RNFL thickness (μM)
GCL+ thickness (μM)
Distance from optic nerve (optic disc diameters)
Orientation from vertical (degrees)
0
100
200
300
400
0.0
0.5
1.0
1.5
2.0
2.5
3.0
60
120
180
240
300
360

Figure 8

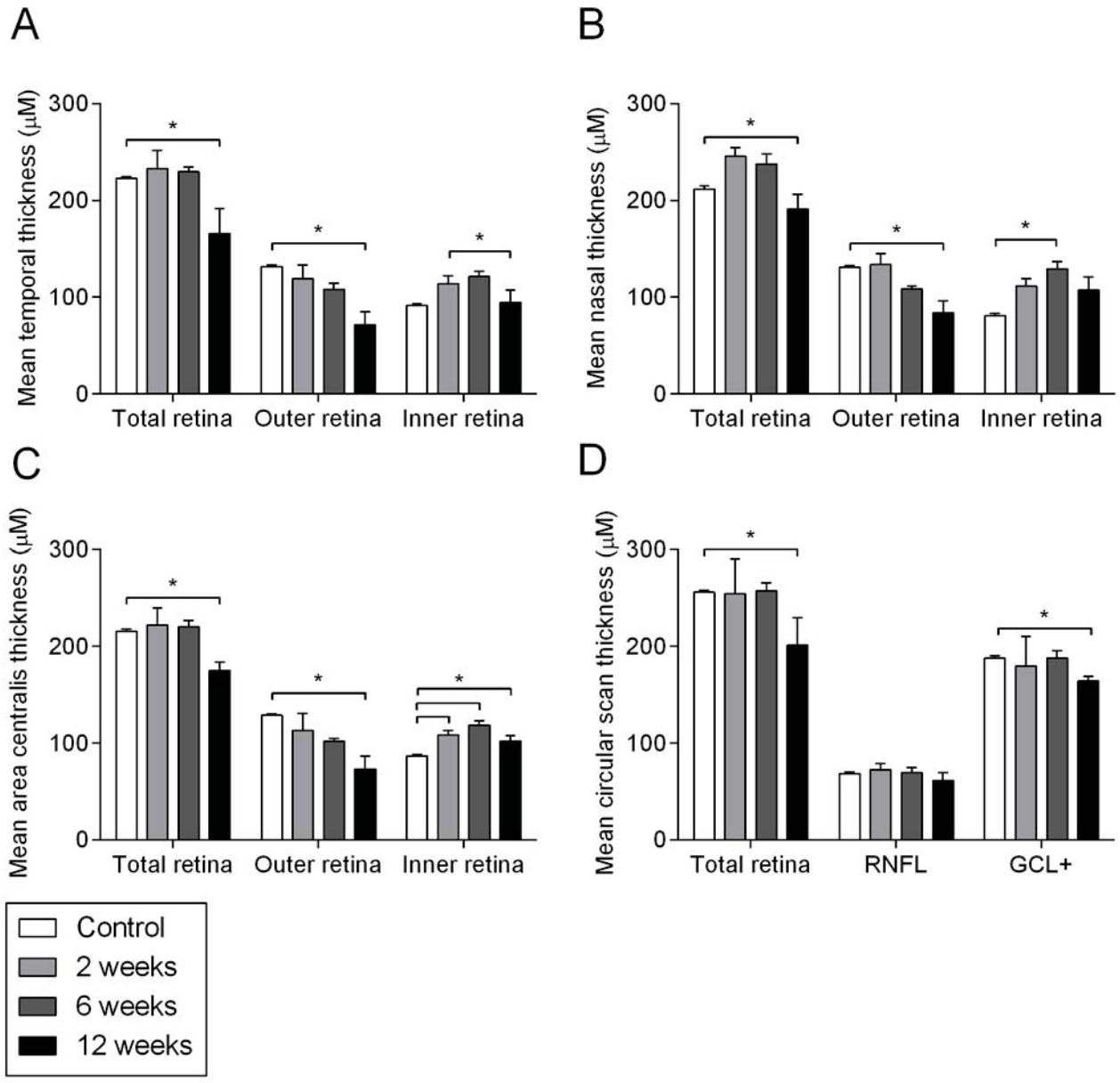
A
Mean temporal thickness (μM)
300
200
100
0
*
*
*
Total retina
Outer retina
Inner retina
B
Mean nasal thickness (μM)
300
200
100
0
*
*
*
Total retina
Outer retina
Inner retina
C
Mean area centralis thickness (μM)
300
200
100
0
*
*
*
Total retina
Outer retina
Inner retina
D
Mean circular scan thickness (μM)
300
200
100
0
*
*
Total retina
RNFL
GCL+
Control
2 weeks
6 weeks
12 weeks

Figure 9